Multiphoton Magnetooptical Trap

Saijun Wu, Thomas Plisson, Roger C. Brown, William D. Phillips, and J. V. Porto
Joint Quantum Institute, NIST and University of Maryland, Gaithersburg, Maryland 20899, USA
(Received 21 August 2009; published 23 October 2009)

We demonstrate a magnetooptical trap (MOT) configuration which employs optical forces due to light scattering between electronically excited states of the atom. With the standard MOT laser beams propagating along the x and y directions, the laser beams along the z direction are at a different wavelength that couples two sets of *excited* states. We demonstrate efficient cooling and trapping of cesium atoms in a vapor cell and sub-Doppler cooling on both the red and blue sides of the two-photon resonance. The technique demonstrated in this work may have applications in background-free detection of trapped atoms, and in assisting laser cooling and trapping of certain atomic species that require cooling lasers at inconvenient wavelengths.

DOI: 10.1103/PhysRevLett.103.173003 PACS numbers: 37.10.De, 32.80.Wr, 37.10.Vz

The development of laser cooling and trapping techniques in the last three decades has greatly enhanced our ability to control atoms, impacting a range of fields from precision atomic measurements and atomic clocks to quantum degenerate gases and quantum information processing. To date, most laser cooling methods use the mechanical effect of single-photon transitions between ground states and electronically excited states. These include Doppler cooling, polarization gradient cooling, and velocity-selective coherent population trapping [1]. There are, however, a few theoretical and experimental studies involving laser cooling in three-level systems comprising a ground state and two electronically excited states. For example, Refs. [2,3] showed an enhancement of radiation pressure by driving a 2-photon transition in a 3-level system. In other work, the effective linewidth for the cooling transition was controlled by dressing the excited state via a coupling to another excited state. This effect can either broaden [4,5] or narrow [6] the effective single-photon cooling transition.

Exploiting the Doppler and Zeeman shifts of single-photon optical dipole transitions, the magnetooptical trap (MOT) [7] has been the standard tool to cool and trap neutral atoms in 3D. The primary motivation of this work is to use Doppler and Zeeman shifts of multiphoton transitions to both cool and trap atoms. We demonstrate a trap geometry where the cooling and trapping of atoms along one axis of the 3D trap is due entirely to optical forces from transitions between two *electronically excited* states [8]. Specifically, with the 852 nm cooling laser beams of a standard cesium (^{133}Cs) MOT propagating along the x and y directions, we replace the laser beams along the z direction with counterpropagating 795 nm laser beams that only couple the excited states of cesium ($6P_{3/2}F' = 5$) to a third set of excited states ($8S_{1/2}F'' = 4$) (see Fig. 1). In this two-color MOT we find efficient cooling along the z direction at both small and large two-photon detunings, while a magnetooptical restoring force was found when the helicities of the $6P$-$8S$ beams are opposite to those for the standard MOT. Remarkably, the two-color MOT can reach sub-Doppler temperatures at both positive and negative two-photon detunings.

The new feature of the two-color MOT sketched in Fig. 1 is in the cooling and trapping along the z direction. Consider the low intensity regime where the rate of excited atoms leaving from both $6P_{3/2}$ and $8S_{1/2}$ states is dominated by spontaneous emission, with negligible contribution from stimulated processes. In this regime, the dominant radiation pressure along $\hat{\mathbf{z}}$ is due to 2-photon scattering, where the first photon is absorbed from the in-plane laser beams and the second is absorbed from the beams along $\hat{\mathbf{z}}$. In particular, we consider $R^{(2)}_{\hat{\mathbf{i}},\hat{\mathbf{j}}}$, the rate of 2-photon scattering induced by a $6S$-$6P$ beam along $\hat{\mathbf{i}}$ and a $6P$-$8S$ beam along $\hat{\mathbf{j}}$. Here $\hat{\mathbf{i}} \in \{\hat{\mathbf{x}}, -\hat{\mathbf{x}}, \hat{\mathbf{y}}, -\hat{\mathbf{y}}\}$ is one of the four directions of the $6S$-$6P$ beams, and $\hat{\mathbf{j}} \in \{\hat{\mathbf{z}}, -\hat{\mathbf{z}}\}$ is one of the two directions of the $6P$-$8S$ beams. The scattering force along $\hat{\mathbf{z}}$ can be written as $\mathbf{f}^{(2)}_z = \hbar k_{ee'} \sum_{\hat{\mathbf{i}},\hat{\mathbf{j}}} R^{(2)}_{\hat{\mathbf{i}},\hat{\mathbf{j}}} \hat{\mathbf{j}}$. For an atom moving at velocity $\mathbf{v}$, we have the 2-photon scattering rate in the low intensity limit:

$$R^{(2)}_{\hat{\mathbf{i}},\hat{\mathbf{j}}} = \frac{\gamma |\Omega_{ge}\Omega_{ee'}|^2}{16|(\tilde{\Delta}_1 - k_{ge}\hat{\mathbf{i}}\cdot\mathbf{v})(\tilde{\delta}_2 - k_{ge}\hat{\mathbf{i}}\cdot\mathbf{v} - k_{ee'}\hat{\mathbf{j}}\cdot\mathbf{v})|^2}. \quad (1)$$

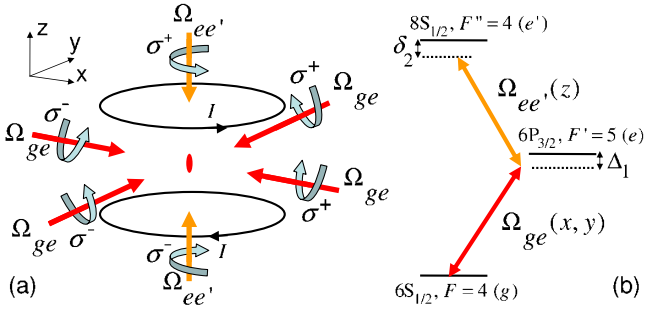

FIG. 1 (color online). (a) Schematic of the setup in this work; $\sigma^{\pm}$ are specified with respect to the positive x, y and z axes. (b) Simplified level diagram and related transitions.

Here Ω_{ge} and $\Omega_{ee'}$ are the Rabi frequencies of the laser induced couplings per beam; k_{ge} and $k_{ee'}$ are the wave numbers of the laser beams; $\tilde{\Delta}_1 = \Delta_1 + i\Gamma/2$ and $\tilde{\delta}_2 = \delta_2 + i\gamma/2$; Δ_1 and δ_2 are the 1-photon and 2-photon detunings for the $6S_{1/2}F = 4$ to $8S_{1/2}F'' = 4$ 2-photon excitation, with $6P_{3/2}F' = 5$ as the intermediate level [Fig. 1(b)]; $\Gamma/2\pi = 5.2$ MHz and $\gamma/2\pi = 1.5$ MHz are the linewidths of the $6P_{3/2}$ and $8S_{1/2}$ states, respectively.

Taylor-expanding Eq. (1) around $v_z = \hat{\mathbf{z}} \cdot \mathbf{v} = 0$ gives $f_z^{(2)} \approx -\alpha^{(2)} v_z$, with $\alpha^{(2)} > 0$ (damping) for negative 2-photon detuning $\delta_2 < 0$. This 2-photon version of the usual [1] Doppler cooling mechanism can be summarized with the level diagram in Fig. 2(a): the Doppler effect enhances the absorption cross section for the $6P$-$8S$ beam opposing the velocity. One qualitative difference from standard Doppler cooling is that the 2-photon transitions to the $8S$ states are not closed, so we expect that repumping light will be important to keep the population from pumping into the $6S_{1/2}F = 3$ ground states.

In addition to the velocity-dependent force, a position-dependent restoring force along the z direction is essential for trapping. Figure. 2(b) illustrates the basic principle of the trapping force. To simplify our discussion, we consider a hypothetical atom with angular momentum $J = 0$ ground state, $J' = 1$ intermediate states, and $J'' = 0$ excited state. As with the cooling force, the trapping force along $\hat{\mathbf{z}}$ is due to the scattering of the $6P$-$8S$ light. The position dependence of this force is due to the spatially dependent Zeeman shift of the *intermediate* $6P_{3/2}$ levels. Taking the quantization axis along $\hat{\mathbf{z}}$, the $6S$-$6P$ beams in the x-y plane provide both σ and π couplings between the ground state and the intermediate states. For a magnetic field along $+\hat{\mathbf{z}}$, [$z > 0$: right side of Fig. 2(b)], the intermediate detuning of the 2-photon excitation is shifted toward resonance for the excitation pathway involving a $\sigma-$ transition to the intermediate state followed by a $\sigma+$ transition to the excited state. As a result, the atoms at $z > 0$ preferentially absorb

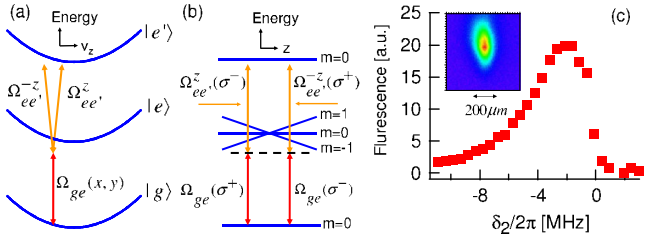

FIG. 2 (color online). (a) Schematic illustration of the velocity damping due to the Doppler effect for 2-photon scattering. Here $\Omega^{\pm z}_{ee'}$ represents the $6P$-$8S$ beam from the $\pm\hat{\mathbf{z}}$ direction. (b) Schematic illustration of the trapping force along z due to the Zeeman shift (z quantization axis) of intermediate resonance in the 2-photon scattering in a linearly changing magnetic field. Only the excitation pathway enhanced by the Zeeman shift is shown. (c) Peak fluorescence of the two-color MOT vs 2-photon detuning δ_2. Here $s_{ge} = 1$, $s_{ee'} = 15$. Inset gives a fluorescence image of the MOT at $\delta_2/2\pi = -3$ MHz.

the $6P$-$8S$ light propagating toward $-\hat{\mathbf{z}}$, leading to a restoring force in a magnetic quadruple field. Unlike the damping force, this restoring force has the correct sign for both positive and negative δ_2 when $\Delta_1 < 0$. In the above analysis we have ignored the ground-state degeneracy in real Cs atoms and thus the associated optical pumping effects [9]. As in a standard MOT [10], efficient cooling and trapping effects associated with optical pumping occur when the Zeeman and Doppler shifts are comparable with the rate of ground-state optical pumping induced by multiphoton excitations.

The predictions of our simple model are corroborated by our experimental observations. In particular, at moderate $6P$-$8S$ intensity the 2-photon detuning must be negative to achieve laser cooling along the z direction of the trap. Surprisingly, at high intensities laser cooling and trapping behave differently. As detailed below, we found laser cooling on both the red and blue sides of the 2-photon resonance. We argue that this counterintuitive effect is due to 3-photon and higher order scattering processes.

Our experiments capture, cool, and trap atoms in a cesium vapor cell. The cooling light in the x-y plane comprises the two pairs of counterpropagating 852 nm laser beams ($6S$-$6P$ beams) with 8 mm $1/e^2$ diameter. (See Fig. 1.) The single-photon detuning $\Delta_1/2\pi = -12.5$ MHz and the peak intensity of each beam is characterized by $s_{ge} \equiv \frac{2\Omega_{ge}^2}{\Gamma^2}$. The gradient of the magnetic quadrupole field was 1.4 mT/cm along $\hat{\mathbf{z}}$. The beams along $\hat{\mathbf{z}}$ are a pair of 795 nm laser beams ($6P$-$8S$ beams), and the peak intensity of each $6P$-$8S$ beam is characterized by the parameter $s_{ee'} \equiv \frac{2\Omega_{ee'}^2}{\gamma^2}$ [11]. We add two counterpropagating repump beams at 895 nm along $\hat{\mathbf{x}}$, tuned to the $6S_{1/2}F = 3$ to $6P_{1/2}F' = 4$ transition to keep atoms in the $F = 4$ ground states.

With the $6P$-$8S$ beams at a moderate intensity of 20 mW/cm^2 ($s_{ee'} \approx 15$, $\Omega_{ee'}/2\pi \approx 4$ MHz), and guided by the 2-photon Doppler cooling picture [Fig. 2(a)], we set the 2-photon detuning δ_2 to small negative values, comparable to the $8S$ linewidth γ. We observe trapped atoms in the two-color MOT when the helicities of the $6P$-$8S$ beams are set to be opposite to those of the $6S$-$6P$ beams in a standard MOT [Figs. 1(a) and 2(b)]. As with a standard MOT [12,13], we find that our trap tolerates wrong helicity components in the $6P$-$8S$ beams with up to $\approx$30% in intensity. As expected, the two-color MOT is more sensitive to the repump efficiency than a standard MOT, and the counterpropagating beams need to be intensity balanced to nullify the repump radiation pressure.

In Fig. 2(c) we plot the peak fluorescence of the two-color MOT vs δ_2. At the optimal 2-photon detuning of $\delta_2/2\pi \approx -3$ Mhz and with $s_{ge} \approx 4$, up to 8×10^5 atoms at a density of 5×10^{10}/cm^3 are accumulated in the two-color MOT from the pressure $P \approx 10^{-5}$ Pascal (10^{-7} Torr) cesium vapor. Because of the weaker trapping and damping along $\hat{\mathbf{z}}$, both the spatial and velocity distri-

butions of the atomic sample are elongated along $\hat{\mathbf{z}}$. The velocity spread of the atoms along $\hat{\mathbf{x}}$ and $\hat{\mathbf{z}}$ is characterized by effective temperatures $T_x \approx 70\ \mu$K and $T_z \approx 700\ \mu$K, both of which are reduced at smaller s_{ge} (see below and Fig. 4). Typical $1/e^2$ widths of the atomic spatial distribution, fit to a Gaussian, are $w_x \approx 300\ \mu$m and $w_z \approx 600\ \mu$m. The number of trapped atoms is an order of magnitude smaller than that of a standard MOT under similar conditions, which is likely due to the reduced capture velocity and effective capture volume for the two-color MOT.

The 2-photon Doppler cooling picture (Fig. 2) fails dramatically at high $6P$-$8S$ beam intensities. As $s_{ee'}$ increases, the range of δ_2 for MOT operation broadens and shifts to the red. When $s_{ee'}$ is larger than a threshold value of $s_{\text{th}} \approx 80$, the two-color MOT also works at positive $\delta_2 > \delta_{\text{th}} \approx 2\pi \times 10\,\text{MHz}$ [Fig. 3(a)]. For $s_{ee'} \approx 1.8 \times 10^3$ (not shown in Fig. 3), the two-color MOT operates for δ_2 spanning a range more than $2\pi \times 100$ MHz ($\gg \gamma, \Gamma$) on both the red and blue sides of the two-photon resonance. The maximum number of trapped atoms is similar to that achieved in the low $6P$-$8S$ beam intensity regimes, but with up to a 50% increase of peak atom densities.

For high $6P$-$8S$ beam intensity and moderate 2-photon detuning, both the spatial and velocity distributions of the trapped atomic sample are more isotropic than those at low intensity. As $s_{ee'}$ increases, the ratio w_z:w_x can reach or even go below unity at small positive δ_2. The ratio T_z:T_x decreases and approaches unity as $s_{ee'}$ increases, while a larger $s_{ee'}$ is needed for the same ratio to be reached at a larger $|\delta_2|$. The effective temperature T_x, and remarkably, also T_z, decrease linearly with s_{ge} until the MOT stops working. For $s_{ge} < 1$, T_z is well below the 125 μK D2 Doppler limit at both large $|\delta_2|$ as well as at small positive 2-photon detunings, as shown in Fig. 4. As in a standard MOT [10], at sub-Doppler temperatures we find the width of the trapped cloud increases with the atom number, indicating effective atom-atom repulsion mediated by fluorescence photons. In addition, at large $|\delta_2|$ the MOT becomes less sensitive to the repump efficiency and intensity balance, as in a standard MOT.

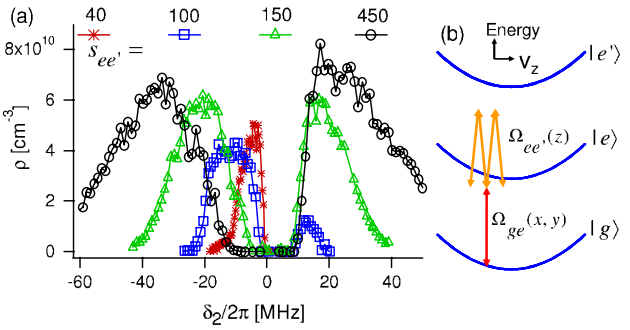

FIG. 3 (color online). (a) Peak atom density vs two-photon detuning δ_2 for atoms in the two-color MOT at different $6P$-$8S$ beam intensities $s_{ee'}$ and for $s_{ge} = 4$. (b) Schematic illustration of the velocity damping due to the Doppler effect for 3-photon scattering.

The observation of laser cooling and trapping on the blue side of the 2-photon resonance is intriguing. Equation (1) indicates that for $\delta_2 > 0$, the Doppler effect leads to a velocity-dependent force that becomes antidamping. At low intensity, this precludes operation of the MOT. However, the 2-photon force picture ignores higher order scattering processes, which can be important at high intensities. These include the 3-photon process sketched in Fig. 3(b) in which a 2-photon absorption is followed by a stimulated emission from $8S$ to $6P$. These multiphoton processes can lead to efficient cooling along $\hat{\mathbf{z}}$ in a manner similar to Doppleron cooling [14]. In the same way as for 2-photon force calculations, the 3-photon scattering force can be written as $\mathbf{f}_z^{(3)} = 2\hbar k_{ee'} \sum_{\hat{\mathbf{i}},\hat{\mathbf{j}}} R^{(3)}_{\hat{\mathbf{i}},\hat{\mathbf{j}},-\hat{\mathbf{j}}} \hat{\mathbf{j}}$, where, for atoms moving at velocity $\mathbf{v}$, the 3-photon scattering rate $R^{(3)}_{\hat{\mathbf{i}},\hat{\mathbf{j}}}$ is

$$R^{(3)}_{\hat{\mathbf{i}},\hat{\mathbf{j}},-\hat{\mathbf{j}}} = \frac{|\Omega_{ee'}|^2}{4|\tilde{\Delta}_1 - k_{ge}\hat{\mathbf{i}} \cdot \mathbf{v} - 2k_{ee'}\hat{\mathbf{j}} \cdot \mathbf{v}|^2} \frac{\Gamma}{\gamma} R^{(2)}_{\hat{\mathbf{i}},\hat{\mathbf{j}}}, \quad (2)$$

with $\tilde{\Delta}_1$ and $R^{(2)}_{\hat{\mathbf{i}},\hat{\mathbf{j}}}$ as in Eq. (1).

As in our treatment of Eq. (1), we Taylor-expand $f_z^{(3)}$ near $v_z = 0$ to find the 3-photon damping coefficient $\alpha^{(3)}$. For $\Delta_1 < 0$ and $\gamma^2 \ll \Gamma^2 + 4\Delta_1^2$, we find $\alpha^{(3)} > 0$ for either $\delta_2 < 0$, or $\delta_2 > -\Delta_1/2$. We note that $\alpha^{(3)}$ involves only the 3-photon process and ignores 2-photon processes, light shifts, and higher order processes. The 3-photon cooling effect at $\delta_2 > 0$ can be understood qualitatively from the diagram in Fig. 3(b): At large $|\delta_2|$, the Doppler sensitivity along $\hat{\mathbf{z}}$ of the $6P$-$8S$-$6P$ Raman process becomes independent of δ_2, but remains dependent on Δ_1. The fact that $\alpha^{(3)}$ is positive is determined by the negative single-photon detuning Δ_1. In addition, the decreased $8S$ population at large $|\delta_2|$ reduces the two-color contribution to unwanted optical pumping into the $F = 3$ ground states, which helps explain the decreased sensitivity on repump light.

There are at least two possible explanations for the sub-$6P_{3/2}$-Doppler temperatures observed along $\hat{\mathbf{z}}$ over the wide range of 2-photon detunings in Fig. 4. First, as with sub-Doppler cooling in standard optical molasses [9], there is an interplay between spatially dependent light shifts and optical pumping among the $6S$ Zeeman sublevels, leading directly to sub-Doppler cooling for atoms moving along $\hat{\mathbf{z}}$. This mechanism may be nonintuitive since the 852 nm light, which is the only light field that interacts with the $6S$ atoms, has no polarization gradient along $\hat{\mathbf{z}}$. However, a z-dependent ground-state spin polarization can be induced by multiphoton optical pumping processes: the $6P$-$8S$ coupling dresses the $6P_{3/2}F' = 5$ Zeeman sublevels, shifting and mixing those sublevels in a z-dependent way. An atom excited to a $6P_{3/2}F' = 5$ dressed state is thus spin polarized, and its z-dependent

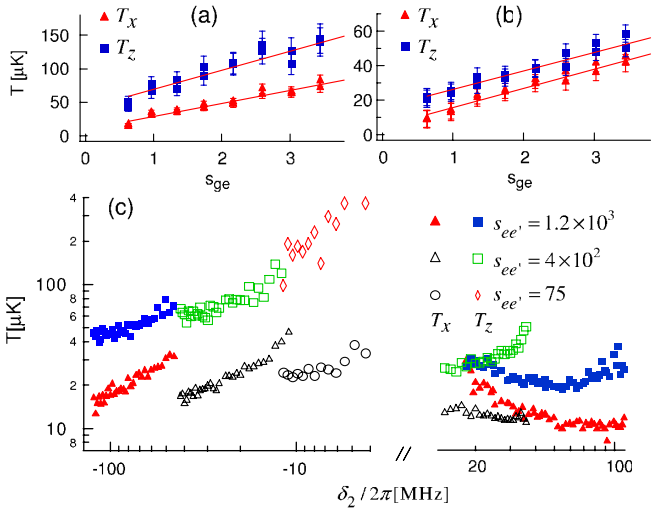

FIG. 4 (color online). (a),(b) Temperature of the atoms vs s_{ge} for $s_{ee'} = 1.8 \times 10^3$, with $\delta_2/2\pi = -143$ MHz in (a) and $\delta_2/2\pi = 117$ MHz in (b). Notice the different temperature scales. (c) Temperature vs δ_2 for atoms in the two-color MOT at various $s_{ee'}$ for $s_{ge} = 0.6$.

polarization is partially retained after the spontaneous decay to the $6S$ ground states. Combined with a light shift of the ground states (due to 2-color processes) which is not only x-, y-dependent but also z-dependent, sub-Doppler cooling can occur along $\hat{\mathbf{z}}$ [15]. The inseparability of the two-color ground-state light shift could also provide a second contribution to the low measured temperature along $\hat{\mathbf{z}}$, by mixing the standard sub-Doppler-cooled motion along $\hat{\mathbf{x}}$, $\hat{\mathbf{y}}$ with the motion along $\hat{\mathbf{z}}$. A quantitative analysis of this "two-color" polarization gradient cooling mechanism will appear in a future publication [16].

We have demonstrated a magneto-optical trap where cooling and trapping forces along its z axis are provided entirely by photons associated with transitions between excited states. Up to 8×10^5 cesium atoms are trapped in a vapor cell, and the density of the trapped atoms reaches $8 \times 10^{10}/\text{cm}^3$ at optimal experimental parameters. Sub-Doppler cooling occurs over a wide range of positive and negative 2-photon detunings. Transferring from a higher-density regular MOT to our MOT, we found the decay of the atom number to be independent of the atom density, up to our highest density of $10^{11}/\text{cm}^3$. The decay from collisions with background gases was 5 s^{-1}. We believe that the number of atoms in the two-color MOT is lower than that in the standard MOT (although the density, for our conditions, are similar), because there is a reduced phase-space volume for capture from the room-temperature vapor. We have also observed atom cooling and trapping with two pairs of 795 nm beams and a single pair of 852 nm beams, either with 852 nm beams in the z direction and 795 nm beams in the x-y plane, or with 852 nm beams in the $x(y)$ direction and 795 nm beams in the $y(x)$-z plane. These schemes trap approximately a factor of 10 fewer atoms than a MOT with only one set of 795 nm beams.

The two-color cooling and trapping demonstrated here may have practical applications. For instance, 852 nm light can be collected along z (a direction unaccessible in the normal MOT configuration) from behind an appropriate filter (mirror). This geometry may be more convenient for approaching a collection solid angle of 2π, while minimizing scattered light. This or similar MOT arrangements may also allow completely background-free detection of fluorescence from atomic transitions driven by no laser beam. As another example, replacing regular cooling lasers with excited-state coupling lasers may be technically advantageous for laser cooling of certain atomic species. For example, for atomic hydrogen or antihydrogen, the Lyman-α cooling transition needs 121 nm coherent radiation, which is hard to generate and manipulate [17,18]. Instead of setting up 3 pairs of Lyman-α beams that couple $1S$ with $2P$ for a regular hydrogen MOT, two pairs of the beams may be replaced by laser beams that couple $2P$ and $3S$ excited states using the more readily available 656 nm light.

We gratefully acknowledge experimental contributions by Jennifer Sebby-Strabley, and helpful discussions with Vincent Boyer and Bruno Laburthe-Tolra.

[1] *Laser Cooling and Trapping*, H. Metcalf and P. van der Straten (Springer-Verlag, Berlin, 1999).
[2] M. Kumakura *et al.*, Jpn. J. Appl. Phys. **31**, L276 (1992).
[3] W. Rooijakkers *et al.*, Phys. Rev. Lett. **74**, 3348 (1995).
[4] T. Binnewies *et al.*, Phys. Rev. Lett. **87**, 123002 (2001).
[5] E. A. Curtis *et al.*, Phys. Rev. A **64**, 031403(R) (2001).
[6] N. Malossi *et al.*, Phys. Rev. A **72**, 051403(R) (2005).
[7] E. L. Raab *et al.*, Phys. Rev. Lett. **59**, 2631 (1987).
[8] This is in contrast to Ref. [6] where the optical force due to excited-state couplings is negligible.
[9] J. Dalibard *et al.*, J. Opt. Soc. Am. B **6**, 2023 (1989).
[10] C. G. Townsend *et al.*, Phys. Rev. A **52**, 1423 (1995).
[11] Ω_{ge} and $\Omega_{ee'}$ are specified for $m_F = 4$–$m_{F'} = 5$ and $m_{F'} = 5$–$m_{F''} = 4$ transitions, respectively. We obtain s_{ge} and $s_{ee'}$ by comparing the intensities of the laser beams with effective saturation intensities of the relevant transitions, with $I_0 = 1.10$ mW/cm^2 for s_{ge} and $I_0 = 1.32$ mW/cm^2 for $s_{ee'}$.
[12] C. Monroe *et al.*, Phys. Rev. Lett. **65**, 1571 (1990).
[13] F. Shimizu *et al.*, Phys. Rev. A **39**, 2758 (1989).
[14] J. J. Tollett *et al.*, Phys. Rev. Lett. **65**, 559 (1990).
[15] The multiphoton optical pumping effect also leads to an enhanced magnetooptical restoring force near the trap center, similar to a standard MOT [10] as shown in our simulations.
[16] R. C. Brown *et al.* (to be published).
[17] I. D. Setija *et al.*, Phys. Rev. Lett. **70**, 2257 (1993).
[18] K. S. E. Eikema *et al.*, Phys. Rev. Lett. **86**, 5679 (2001).